J Mater Sci: Mater Med (2006) 17:583–596
DOI 10.1007/s10856-006-9220-z

Kinetics and mechanisms of the conversion of silicate (45S5), borate, and borosilicate glasses to hydroxyapatite in dilute phosphate solutions

Wenhai Huang · Delbert E. Day · Kanisa Kittiratanapiboon · Mohamed N. Rahaman

Received: 25 July 2005 / Accepted: 23 August 2005

Abstract Bioactive glasses with controllable conversion rates to hydroxyapatite (HA) may provide a novel class of scaffold materials for bone tissue engineering. The objective of the present work was to comprehensively characterize the conversion of a silicate bioactive glass (45S5), a borate glass, and two intermediate borosilicate glass compositions to HA in a dilute phosphate solution at 37°C. The borate glass and the borosilicate glasses were derived from the 45S5 glass by fully or partially replacing the SiO_2 with B_2O_3. Higher B_2O_3 content produced a more rapid conversion of the glass to HA and a lower pH value of the phosphate solution. Whereas the borate glass was fully converted to HA in less than 4 days, the silicate (45S5) and borosilicate compositions were only partially converted even after 70 days, and contained residual SiO_2 in a Na-depleted core. The concentration of Na^+ in the phosphate solution increased with reaction time whereas the PO_4^{3-} concentration decreased, both reaching final limiting values at a rate that increased with the B_2O_3 content of the glass. However, the Ca^{2+} concentration in the solution remained low, below the detection limit of atomic absorption, throughout the reaction. Immersion of the glasses in a mixed solution of K_2HPO_4 and K_2CO_3 produced a carbonate-substituted HA but the presence of the K_2CO_3 had little effect on the kinetics of conversion to HA. The kinetics and mechanisms of the conversion process of the four glasses to HA are compared and used to develop a model for the process.

W. Huang · D. E. Day · M. N. Rahaman
Materials Research Center, University of Missouri-Rolla, 101 Straumanis Hall, Rolla, MO 65409

W. Huang
School of Materials Science and Engineering, Tongji University, Shanghai, 200092, China

D. E. Day · M. N. Rahaman (✉)
Department of Materials Science and Engineering, University of Missouri-Rolla, 222 McNutt Hall, Rolla MO 65409-0340
Tel.: 573-341-4406
e-mail: rahaman@umr.edu

K. Kittiratanapiboon
Center for Environmental Science and Technology, University of Missouri-Rolla, 105 USBM, Rolla, MO 65409

1. Introduction

Since the report of its bone-bonding properties in 1971 by Hench *et al.* [1], the silicate-based bioactive glass codenamed 45S5, and referred to as Bioglass®, with a typical composition of 45% SiO_2, 24.5% Na_2O, 24.5% CaO, and 6% P_2O_5 (by weight), has been of primary interest for biological applications [2–5]. Later studies revealed that several silicate-based glasses and glass-ceramics also have the ability to enhance bone formation and bond to surrounding tissue [2–13]. Whereas the low chemical durability of some borate glasses has been known for decades, it is only very recently that the potential of borate glasses in biomedical applications has been explored [14–16]. A borate glass, designated 45S5B1, with the same composition as 45S5 glass but with all the SiO_2 replaced with B_2O_3, was investigated by Richard [17], who found that a hydroxyapatite (HA) layer formed on the borate glass surface upon immersion in a K_2HPO_4 solution at 37°C. Furthermore, the HA layer formed more rapidly on the borate glass than on 45S5 glass. In a preliminary *in vivo* experiment, 45S5B1 glass particles (partially reacted in K_2HPO_4 solution to produce a HA surface layer) were found to promote bone formation more rapidly than 45S5 glass particles upon implantation into tibial defects in rats [17]. A borate glass with a composition somewhat similar

to 45S5B1 was recently found to support the growth and differentiation of human mesenchymal stem cells [18].

The rapid conversion of borate glasses to HA at near body temperature and its apparently favorable *in vitro* and *in vivo* reaction to cells and tissues appear promising but a more detailed characterization is required in order to assess the potential of borate glasses for biomedical applications. An important characteristic of bioactive glasses is the time-dependent modification of the surface, leading to the formation of a HA layer that bonds to the surrounding tissue [19, 20]. It has been suggested that the formation of a HA layer *in vitro* is indicative of a material's bioactive potential *in vivo* [21]. For 45S5 bioactive glass, key steps in the conversion to HA has been described by Hench [4, 5] but many details of the chemical and structural changes that accompany the conversion are not clear. It is well established that that an initial step in the reaction is the formation of a SiO_2-rich gel on the 45S5 glass surface by ion exchange reactions. Further dissolution of ions from the glass and their diffusion through the SiO_2-rich gel layer, followed by the reaction between Ca^{2+} ions from the glass and PO_4^{3-} ions from the surrounding liquid, leads to the growth of HA on the gel layer. The conversion of borate glasses to HA appears to follow a process similar to that for 45S5 glass, but without the formation of a SiO_2-rich layer [22]. However, details of the reaction kinetics and mechanism, as well as the chemical and structural changes occurring during the conversion are not clear.

The objective of the this work was to comprehensively characterize the conversion of four glasses, a silicate bioactive glass (45S5), a borate equivalent of 45S5 glass formed by replacing all the SiO_2 in 45S5 glass with B_2O_3, and two intermediate borosilicate glass compositions, to HA in a dilute (0.02 M) K_2HPO_4 solution at 37°C. Weight loss and pH changes accompanying the conversion were measured, and a variety of techniques were used to characterize the structural and chemical changes. The data were used to provide additional insight into the kinetics and mechanisms of the conversion of bioactive silicate glasses, borate glasses, and intermediate borosilicate compositions to HA. The results are applicable to the development of bioactive glasses that have controllable conversion rates to HA, which may provide a novel class of scaffold materials for bone tissue engineering.

2. Experimental

2.1. Preparation of glasses

Four different glass compositions were used in the experiments. One was the silicate-based 45S5 bioactive glass (designated in this work as 0B). Another glass (designated 3B), a so-called borate equivalent of 45S5 glass which was studied by Richard [17], had the same composition as 45S5 glass but with all the SiO_2 replaced with B_2O_3. The two remaining glasses had intermediate borosilicate compositions between 0B and 3B, with 1/3 and 2/3 of the SiO_2 molar concentration in 45S5 replaced with B_2O_3 (designated 1B and 2B, respectively). The compositions of these four glasses are given in Table I.

The glasses were prepared by melting the required quantities of SiO_2 (Fused quartz; Particle Processing & Classifying Corp., Patterson, NJ), H_3BO_3, $CaCO_3$, Na_2CO_3, and $NaH_2PO_4 \bullet 2H_2O$ (Reagent grade; Fisher Scientific; St. Louis, MO) in a platinum/rhodium crucible in air for 2 h at 1100°C for compositions 2B and 3B, at 1200°C for 1B, and at 1300°C for 0B. The melt was stirred twice at the isothermal temperature and quenched between two steel plates. Each glass was crushed in a hardened steel mortar and pestle to form particles, which were sieved through stainless steel sieves to produce particles with three different size ranges for the experiments: 150–300, 300–500, and 500–1000 μm.

2.2. Phosphate solution for conversion reaction

The phosphate solution used in the conversion of the glasses to HA was prepared by dissolving K_2HPO_4 (Reagent grade; Fisher Scientific, St. Louis MO) in deionized water (pH = 5.5 ± 0.1) to give a solution with a 0.02 M concentration of K_2HPO_4 and with a pH value of 7.0 ± 0.1. The K_2HPO_4 concentration was chosen on the basis of the quantities of glass particles and solution used in the experiments (1 g glass in 100 cm^3 solution), with the requirement that sufficient PO_4^{3-} ions would be available in the solution to react with all the Ca^{2+} ions from the glass to form stoichiometric HA [$Ca_{10}(PO_4)_6(OH)_2$]. In fact, the K_2HPO_4 concentration was chosen to leave a small concentration (200–300 ppm) of residual PO_4^{3-} ions in the solution if the conversion reaction went to completion. This ensured that the Ca^{2+} content of the glass was the only compositional factor that could limit the completion of the reaction. The pH of the starting solution was adjusted to 7.0, which is approximately equal to that of human body fluid, by adding a few drops of dilute HCl.

In a separate set of experiments, the conversion of each glass was carried out under the same conditions but in a mixed solution containing 0.02 M K_2HPO_4 and 0.02 M K_2CO_3 (Fisher Scientific, St. Louis, MO) to study the formation of HA containing CO_3^{2-} ions, since a carbonate-substituted HA is more commonly found in human bone.

2.3. Weight loss and pH measurements

The conversion of silicate and borate glasses to HA in a phosphate solution is accompanied by a decrease in the mass of the glass, so weight loss measurements provide a useful parameter for monitoring the kinetics of the conversion reaction. A reaction system consisting of 1 g of glass in 100 cm^3

Table 1 Compositions of the four glasses used in the experiments

	Mole percent					Weight percent				
Glass	Na_2O	CaO	B_2O_3	SiO_2	P_2O_5	Na_2O	CaO	B_2O_3	SiO_2	P_2O_5
0B	24.4	26.9	0	46.1	2.6	24.5	24.5	0	45.0	6.0
1B	24.4	26.9	15.4	30.7	2.6	24.0	23.9	17.0	29.3	5.8
2B	24.4	26.9	30.7	15.4	2.6	23.4	23.4	33.1	14.4	5.7
3B	24.4	26.9	46.1	0	2.6	22.9	22.9	48.6	0	5.6

solution was used in all the conversion experiments. Prior to the conversion process, the glass particles were washed ultrasonically three times with deionized water, then twice with ethanol, and dried overnight at 90°C. The mass of glass particles was measured to an accuracy of ± 0.01 mg and placed in a cylindrical polyethylene container, the bottom of which consisted of a nylon screen (mesh size = 5 μm) to permit circulation of the solution but to prevent loss of the glass particles and reaction products from the container. The cylinder containing the glass particles was suspended near the center of the phosphate solution contained within a 125 cm^3 polyethylene bottle, and the system was placed in an oven at 37 ± 2°C. During the reaction process, the system was removed from the oven at regular intervals and vibrated for 30 s each time to prevent the glass particles from sticking together.

Weight loss measurements were made after removing the container with the glass particles from the phosphate solution, washing the particles three times with deionized water, and drying for more than 12 h at 90°C. The weight loss was taken as the difference between the initial (unreacted) mass of particles and the mass at time *t*.

The conversion of the glasses to HA in a phosphate solution is also accompanied by changes in the ionic concentrations of the solution, resulting from dissolution of components (e.g., Na_2O, B_2O_3, SiO_2) from the glass into the solution, and precipitation of PO_4^{3-} from the solution to form HA. These changes in ionic concentration influence the pH of the solution, so the pH was also monitored during the conversion reaction. After removing the glass particles from the phosphate solution for the weight loss measurement at time *t* (described above), the solution was cooled to room temperature and its pH value was measured using a pH meter (Accumet-AR25; Fisher Scientific, St Louis, MO).

2.4. Structural and chemical characterization of the reacted glass

Structural and compositional changes in the glasses which resulted from the reaction with the phosphate solution were monitored using several techniques. Scanning electron microscopy (SEM) coupled with energy-dispersive X-ray analysis (EDS) in the SEM (Hitachi: S-4700) were used to investigate structural and compositional changes in the reacted glass. Crystalline phases were detected by X-ray diffraction (XRD; Scintag 2000) using Cu K_α radiation (λ = 0.15406 nm) in a step-scan mode (0.05° per step) in the range of 10–80° 2θ. Compositional analysis of the unreacted glasses and the reaction products was performed using X-ray fluorescence (XRF; XEPOS, Spectro Analytic, Marbough, MA). Fourier transform infrared (FTIR) analysis (Perkin Elmer 1760-X) of the reacted glasses was performed in the wavenumber range of 400–4000 cm^{-1} on disks prepared from a mixture of 2 mg of the reacted glass with 150 mg of high-purity grade KBr. The spectra were corrected by subtracting the KBr spectrum.

2.5. Chemical analysis of the reaction solution

Changes in the ionic concentrations of the phosphate solution which resulted from the conversion reaction were measured using atomic absorption (AA) spectroscopy (Perkin Elmer Model 3100) and ion chromatography (IC; Dionex Series 4000i with conductivity detector). After a given time of reaction between the glass and the phosphate solution, 1 cm^3 of the solution was removed for analysis. The concentrations of Na^+ and Ca^{2+} ions in the solution were measured using AA, whereas the PO_4^{3-} concentration was measured using IC. The IC measurements were conducted by using 2.7 mM Na_2CO_3 and 0.3 mM $NaHCO_3$ as fluent through the column of the Dionex IonPac (AS12A; 4 mm) at a flow rate of 1.5 cm^3/min with the isocratic program.

3. Results and discussion

3.1. Weight loss and pH changes during the conversion reaction

Fig. 1 shows the fractional weight loss, ΔW, versus reaction time, *t*, for particles (150–300 μm) of the four glass compositions during conversion to HA in 0.02 M K_2HPO_4 solution. [$\Delta W = (W_o - W)/ W_o$], where W_o is the initial mass and W is the mass at time *t*.) For each glass, ΔW increased with time, eventually reaching a final limiting value, ΔW_{lim}. The attainment of ΔW_{lim} was taken as an indication of the completion

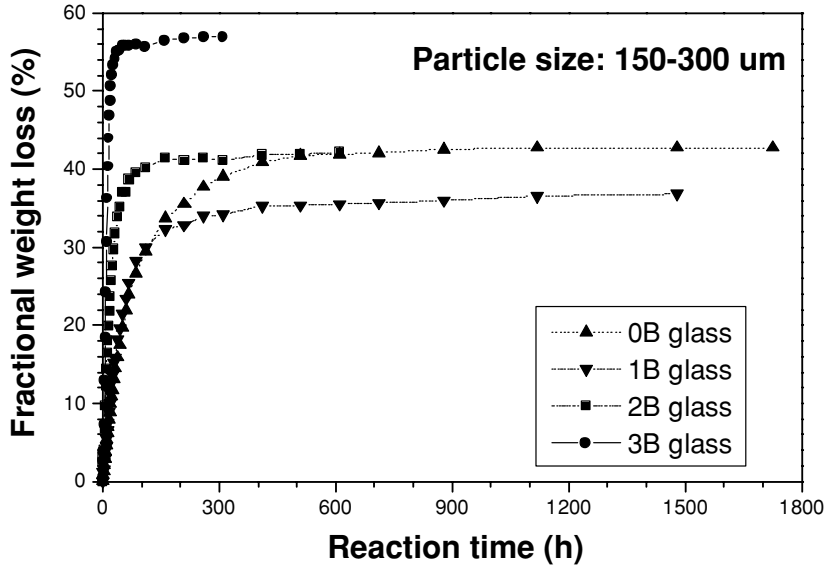

Fig. 1 Weight loss versus time during the conversion of silicate (0B), borate (3B), and borosilicate (1B, 2B) glass particles (150–300 μm) to HA in 0.02 M K_2HPO_4 solution at 37°C.

of the reaction and the inverse of the time required to reach ΔW_{lim} was taken as a measure of the reaction rate. The data showed that the reaction rate increased with increasing B_2O_3 content of the glass. The difference in reaction rate between the 0B and 3B glasses was very remarkable, with ΔW reaching its limiting value in < 60 h for 3B, compared with > 600 h for 0B. The value of ΔW_{lim} did not increase systematically with B_2O_3 content, being highest for 3B (∼60%) and lowest for 1B (∼35%), with the values for 0B and 2B being approximately the same (∼40%). The particle size (150–300, 300–500, and 500–1000 μm) of the glass had only a weak effect on the weight loss kinetics for the 2B and 3B glasses, but as shown in Figs. 2(a) and 2(b), the particle size effect was significant for the 0B and 1B glasses, particularly in the earlier stages of the conversion.

Fig. 3 shows data for the pH of the phosphate solution as a function of reaction time for the four glasses with a particle size of 150–300 μm. The starting pH value of the solution was 7.0 for all four systems. The pH increased rapidly with time, eventually reaching a nearly constant value. With increasing B_2O_3 content of the glass, the pH of the solution increased more rapidly with time, reaching a final limiting value at a shorter time, but the final limiting pH value was lower. For the 0B glass sample, a final pH value of 11.5 was reached after ∼500 h, whereas it took only ∼50 h to reach the final pH of 9.6 for the 3B glass. The data show that quite high pH values

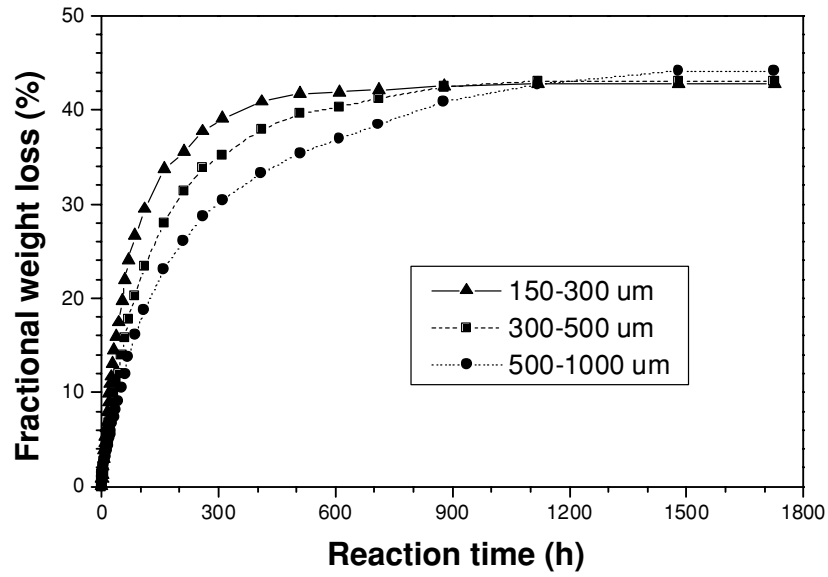

(a)

Fig. 2 Effect of particle size on the conversion of (a) silicate (0B) glass, and (b) borosilicate (1B) glass to HA in 0.02 M K_2HPO_4 solution at 37°C.

Fig. 2 Continued

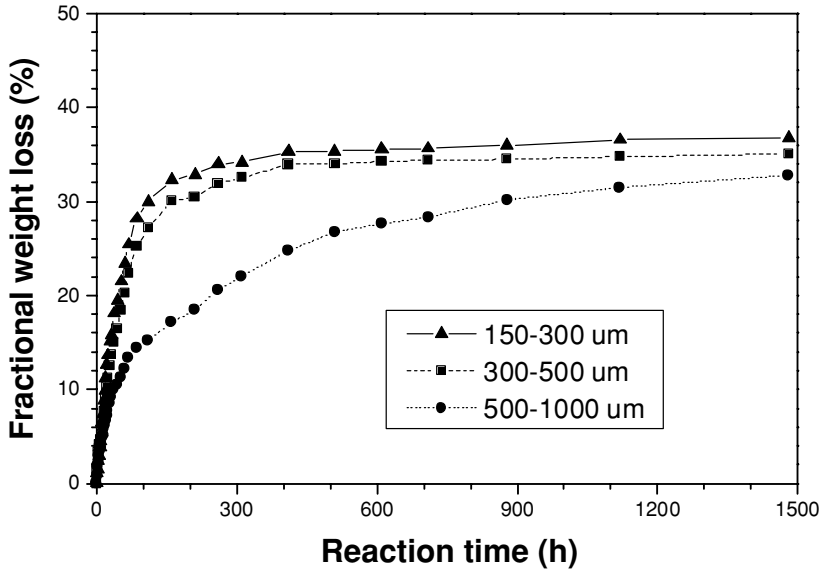

(b)

are reached when silicate and borate bioactive glasses are converted to HA in a static or intermittently-stirred phosphate solution. For each glass, the effect of particle size on the solution pH was measured but the data indicated only a very weak effect.

The increase in pH results from differences in the acidity and basicity of the ionic species involved in the solution-precipitation reactions that occur during the conversion process. Components in the glass such as Na_2O, SiO_2, and B_2O_3 dissolve into the solution to form Na^+, BO_3^{3-}, and SiO_4^{4-} ions, whereas Ca^{2+} ions from the glass react with PO_4^{3-} from the solution to precipitate HA. The strongly basic NaOH overwhelms the weak acidic tendency of $B(OH)_3$ and $Si(OH)_4$, so the pH increases. The rate of increase of the solution pH is controlled by the rate of the solution-precipitation reactions during the conversion to HA. A higher B_2O_3 content gives a glass with lower chemical durability which reacts faster with the solution, so the pH increases faster. The value of the final, limiting pH is controlled by the acidity and basicity of the ions released into the solution as well as their concentrations. When all the Na_2O has dissolved, the solution should reach its final, limiting pH. Since $B(OH)_3$ has a stronger acidic tendency than $Si(OH)_4$, an increase in the B_2O_3 content of the glass leads to a lower final pH.

During the conversion to HA, the reactions that lead to weight loss of the glass are also the same reactions that control the pH of the solution, so it may be expected that the weight loss and pH data would show approximately the same

Fig. 3 pH of the phosphate solution versus time during the conversion of glasses 0B, 1B, 2B, and 3B to HA in 0.02 M K_2HPO_4 solution at 37°C.

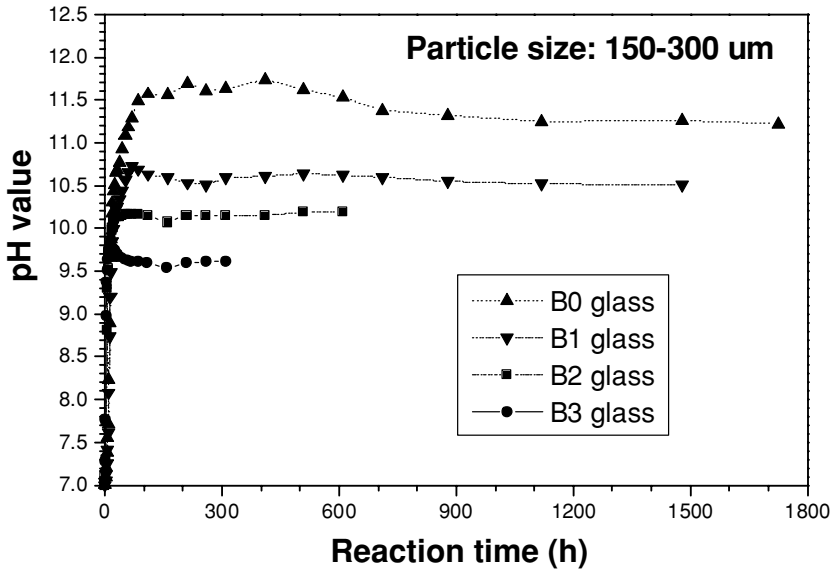

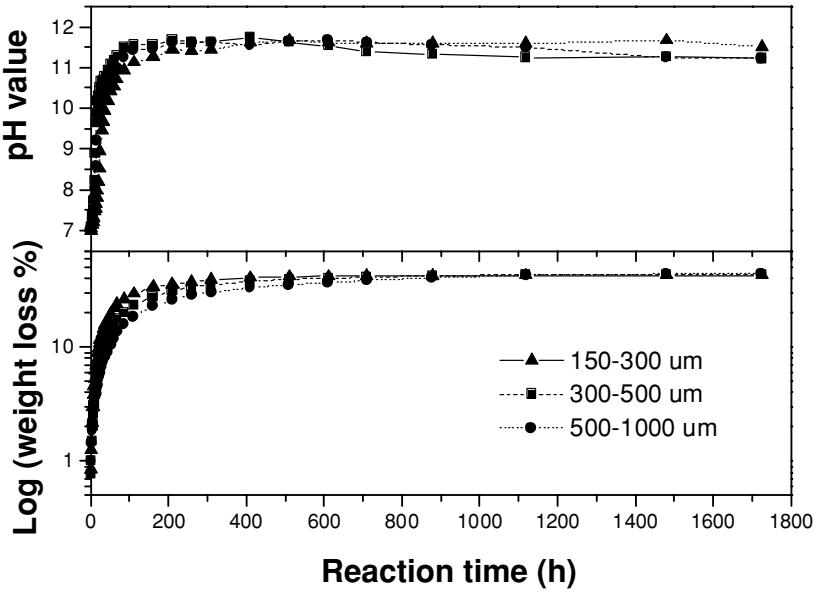

Fig. 4 Plots of the weight loss and solution pH for the conversion of silicate (0B) glass to HA, showing a similar dependence with reaction time.

time dependence. The data in Fig. 4 show that this is indeed so. The weight loss and pH curves have similar shapes, and they both approach limiting values at approximately the same time.

3.2. Structural and chemical changes in the glass resulting from conversion to HA

XRD patterns of the final product of the four glasses, after reaction in the phosphate solution, are shown in Fig. 5. The major peaks in the patterns corresponded to those of a standard HA, $Ca_{10}(PO_4)_6(OH)_2$ (JCPSD 72-1243), indicating the formation of HA during the reaction. The diffraction peaks in the patterns of the reaction products were broad and relatively weak in intensity when compared to those of the standard, which may be an indication that the as-formed HA product had not fully crystallized or that the crystallite size of the HA product was in the nanometer range, or a combination of both. The data also showed the formation of an HA product for all four glasses, indicating that the presence of SiO_2 or B_2O_3 did not affect the ability to form HA (although the *rate* of formation is dependent on the composition, as described above).

Fig. 6 shows FTIR spectra of the final products for the four glasses after reaction in the phosphate solution, along with the spectrum for a commercial HA powder (Ceramic Hydroxyapatite, Bio-Rad Labs., Hercules, CA). Whereas the spectra for all four glasses showed the major resonances associated with HA, at wavenumbers of 560 and 605 cm^{-1} characteristic of the P–O resonance in PO_4^{3-} [23], minor differences were also apparent. The peak at 870 cm^{-1} in the spectra was attributed to the P–O–H resonance in HPO_4^{2-} [24], whereas

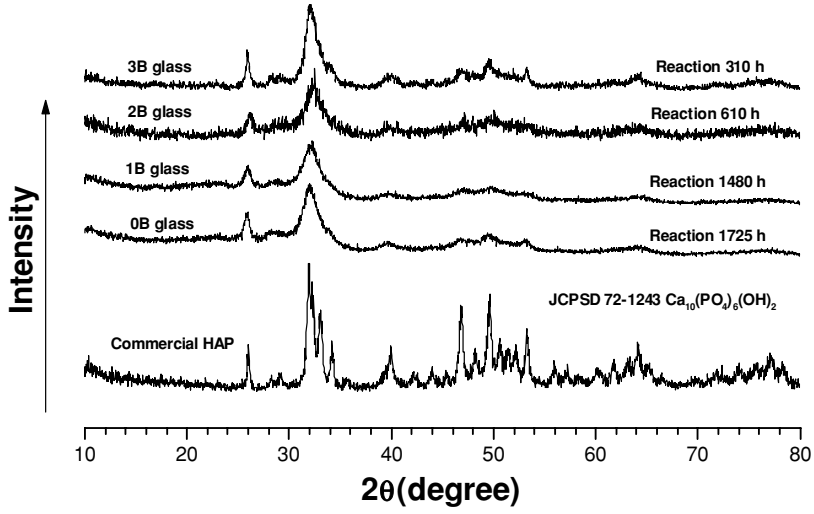

Fig. 5 XRD patterns of the products for the 0B, 1B, 2B, and 3B glasses, after reaction in 0.02 M K_2HPO_4 solution at 37°C for the times shown. The patterns are for the "as-formed" HA. For comparison, the pattern for a standard HA is also shown.

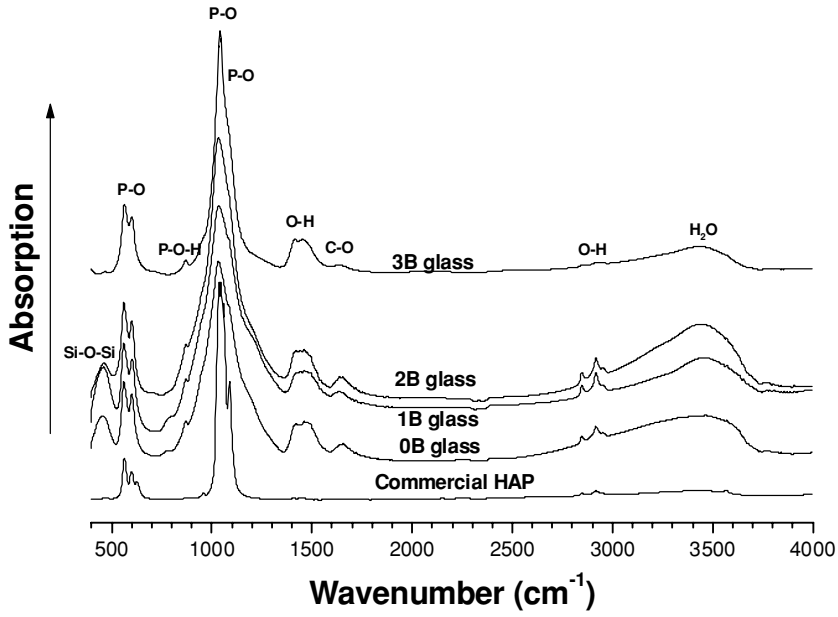

Fig. 6 FTIR spectra of the products for the 0B, 1B, 2B, and 3B glasses, after reaction in 0.02 M K_2HPO_4 solution at 37°C for the times shown. For comparison, the spectrum for a commercial HA is also shown.

the peaks at 1414, 1550, and 1640 cm^{-1} were attributed to the C–O resonance in CO_3^{2-} [25]. The FTIR spectra therefore indicated the presence of some HPO_4^{2-} and CO_3^{2-} in the HA formed from the glasses.

The HPO_4^{2-} presumably substituted for PO_4^{3-} groups in the HA lattice, with a corresponding deficiency in Ca^{2+} to maintain electroneutrality. The formation of a Ca-deficient HA, reported to be kinetically more favorable than the formation of stoichiometric HA [26], would make the Ca/P atomic ratio smaller than 1.67. In the present work, the reaction was limited only by the availability of Ca^{2+} ions from the glass, leading to conditions that are expected to be favorable for the incorporation of HPO_4^{2-} into the HA structure. Since the present experiments were carried out in air, it is likely that CO_2 from the atmosphere dissolved into the solution, giving rise to the substitution of CO_3^{2-} into the lattice. While the substitution of PO_4^{3-} in the HA lattice by CO_3^{2-} is commonly observed [27, 28], it has been reported that CO_3^{2-} can also substitute for OH^- when the HA is precipitated in a solution containing CO_3^{2-} ions [29].

The FTIR spectra in Fig. 5 show a resonance at 450 cm^{-1}, attributed to the Si–O bending vibration in SiO_4^{4-} [13], for the products of the 0B, 1B, and 2B glasses only, and not for the product of the 3B glass, indicating the presence of residual silicate species in the reaction products of the 0B, 1B, and 2B glasses.

SEM of the final reacted particles (deliberately broken to reveal cross-sections) indicated that the HA reaction product had a layered structure as shown for the 0B and 3B compositions in Figs 7(a) and 7(c). Since these samples were identical to those used in the weight loss experiments, the layers were presumably caused by removing the samples from, and re-inserting them into the solution at periodic intervals during the weight loss experiments. Higher magnification micrographs revealed that the HA product from all four glasses consisted of a porous, fine-grained structure, with pore sizes on the order of nanometers. Some differences in the morphology of the HA product were also apparent, as shown in Figs 7(b) and 7(d) for the 0B and 3B glasses.

EDS analysis of the final reaction products indicated compositional differences that depended on the composition of the initial glass (Table 2). For the 3B glass, the major oxide components in the product were CaO and P_2O_5. The Ca/P atomic ratio was 1.7, close to the value (1.67) for stoichiometric HA, indicating almost complete conversion of the 3B glass to HA. In comparison, the reaction products for the 0B, 1B, and 2B glasses were composed predominantly of CaO, SiO_2, and P_2O_5. The concentration of B_2O_3, if any, could not be accurately determined because of the insensitivity of this technique for low atomic number elements. The data indicated incomplete conversion of the 0B, 1B, and 2B glasses to HA, with residual SiO_2 in the reaction product. For all four glasses, no detectable amount of Na_2O was found in the reaction products.

Table 2 also gives the XRF data for the compositions of the final products for the four glasses after reaction in the phosphate solution. (The XRF data are in parentheses.) The presence of B_2O_3, if any, could not be accurately determined because of the insensitivity of XRF for low atomic number elements. As found in the EDS analysis, for all four glasses, there was no detectable amount of Na_2O in the reaction products. For the 3B glass, the reaction product consisted only of CaO and P_2O_5. The composition and the Ca/P atomic ratio (1.7) were almost identical to those measured using EDS. The

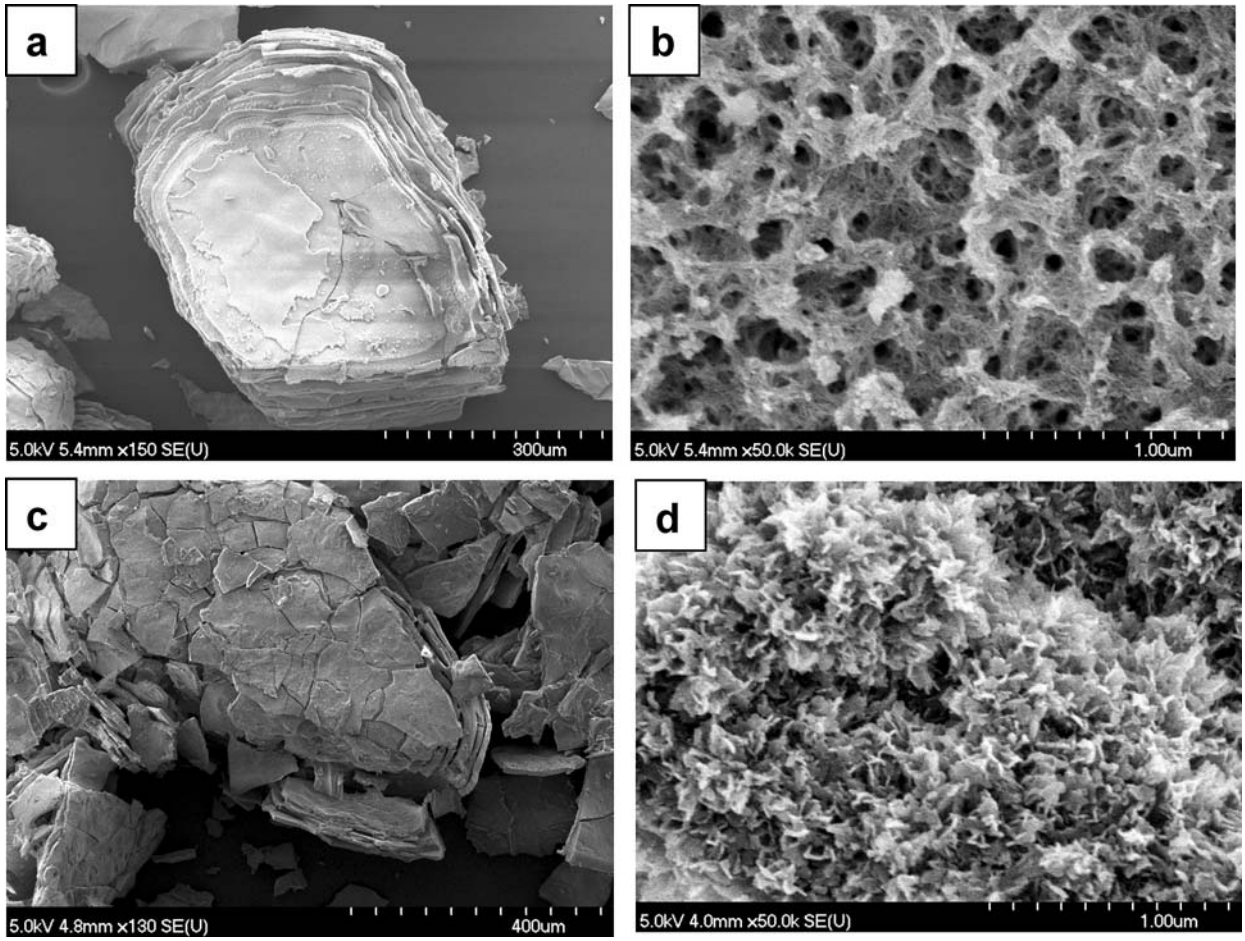

Fig. 7 SEM of the reaction products for the silicate 0B glass (a) and the borate 3B glass (c). The particles were deliberately broken to show the internal structure. Higher magnification micrographs of the surfaces of the reaction products for 0B glass (b) and 3B glass (d), showing a porous structure with fine pores.

reaction products for the 0B, 1B, and 2B glasses contained a significant fraction of residual SiO_2, indicating incomplete conversion to HA.

It is seen from Table 2 that differences existed between the XRF and EDS data for the reaction products of the 0B, 1B, and 2B glasses. These products contain more than one phase, and the differences between the EDS and XRF data result largely from the methodology inherent to each technique. XRF gives the overall composition of a representative sample of the product. On the other hand, the EDS data are an average of several local compositions which are dependent on the positions at which the analysis is performed.

The chemical data obtained from EDS and XRF of the reaction products consistently show that the borate (3B) glass was fully converted to HA, whereas the silicate (0B) and borosilicate (1B and 2B) glasses were only partially converted to HA, with an unconverted core containing a significant amount of SiO_2 but no Na_2O.

Table 2 EDS and XRF data for the compositions of the reaction products (in wt%) and the Ca/P atomic ratios, for the four glasses after conversion to HA in a dilute phosphate solution. (The XRF data are in parentheses.)

Glass	SiO_2	CaO	P_2O_5	Ca/P
0B	47.3 (30.0)	32.8 (45.2)	19.9 (24.8)	2.1 (2.3)
1B	34.6 (38.3)	40.9 (41.0)	24.5 (20.7)	2.1 (2.5)
2B	37.5 (25.6)	36.2 (48.1)	26.4 (26.3)	1.8 (2.3)
3B	0 (0)	57.3 (57.3)	42.7 (42.9)	1.7 (1.7)

3.3. Ionic concentrations in the phosphate solution

For all four glass compositions, the Na^+ concentration in the phosphate solution increased with reaction time, due to Na dissolution from the glass, and eventually reached a final limiting value (Fig. 8). The initial rate of increase of the Na^+ concentration was dependent on the composition of the glass, being more rapid for higher B_2O_3 content of the glass. Whereas the final limiting Na^+ concentration was only weakly dependent on the glass composition, the data

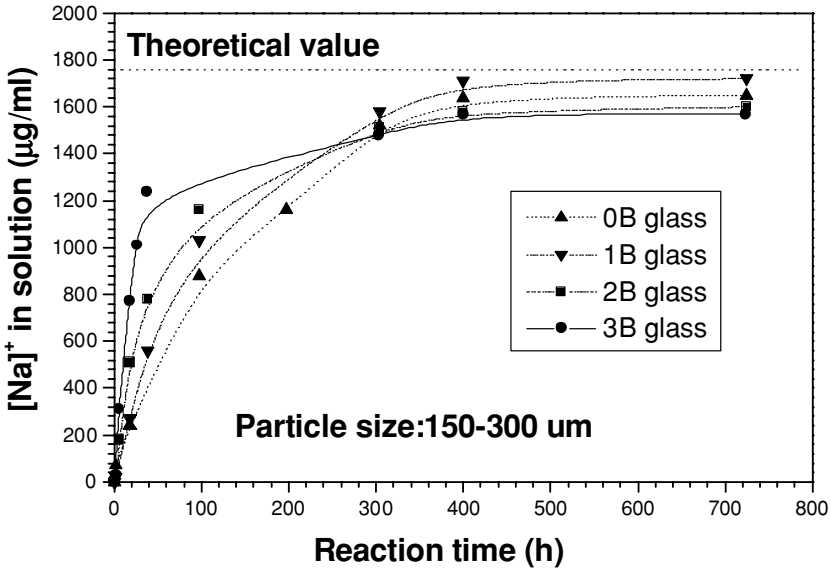

Fig. 8 Sodium ion concentration versus reaction time for the solutions resulting from the conversion reactions with glasses 0B, 1B, 2B, and 3B.

indicated a small increase with decreasing B_2O_3 content of the glass, presumably due to the slightly higher concentration (by weight) of Na_2O in the glass with increasing decreasing B_2O_3 content (see Table I). Assuming that all the Na_2O in the glass dissolved completely into the phosphate solution, the theoretical Na^+ concentration in the solution was calculated to be 1700–1820 μg/cm^3. The data indicated that the measured value was approximately equal to the theoretical value for all four glasses, with the deviation from the theoretical value being less than 8%.

The AA data for the solution, along with the EDS and XRF data of the reaction product consistently show that all the Na in the glass dissolves into the solution during the conversion process, regardless of the composition of the glass and regardless of whether the glass was fully or partially converted to HA.

Fig. 9 shows data for the time dependence of the PO_4^{3-} concentration in the solution resulting from the reactions with the four glasses. The concentration decreased with time, due to reaction with Ca^{2+} to precipitate HA, eventually reaching a final limiting value. The initial rate at which the PO_4^{3-} concentration decreased was found to depend on the B_2O_3 content of the glass, being most rapid for the 3B glass with the highest B_2O_3 content. The initial HPO_4^{2-} concentration in the 0.02 M K_2HPO_4 solution was 1930 μg/cm^3 but only part of the HPO_4^{2-} was converted to PO_4^{3-} at the starting pH of 7.0. The measured PO_4^{3-} concentration in the initial solution was 850 μg/cm^3. If the PO_4^{3-} ions reacted with all

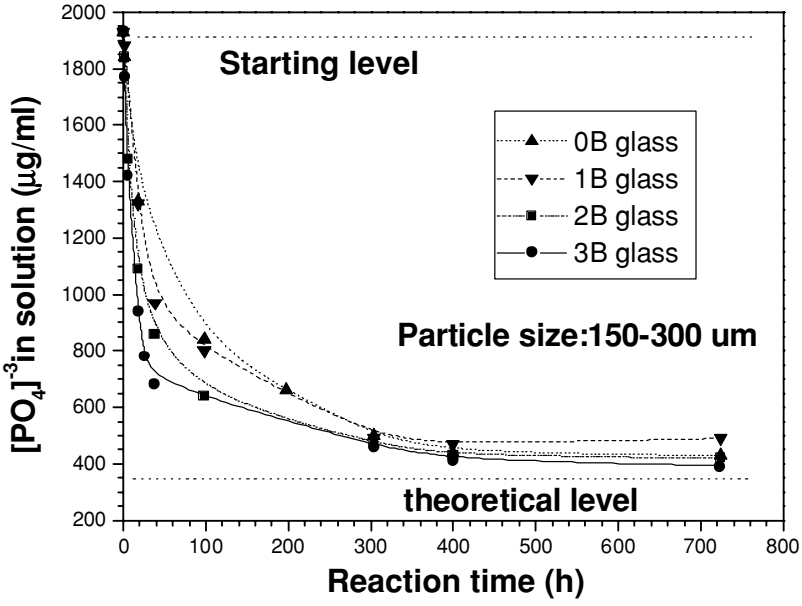

Fig. 9 Phosphate ion concentration versus reaction time for the solutions resulting from the conversion reactions with 0B, 1B, 2B, and 3B.

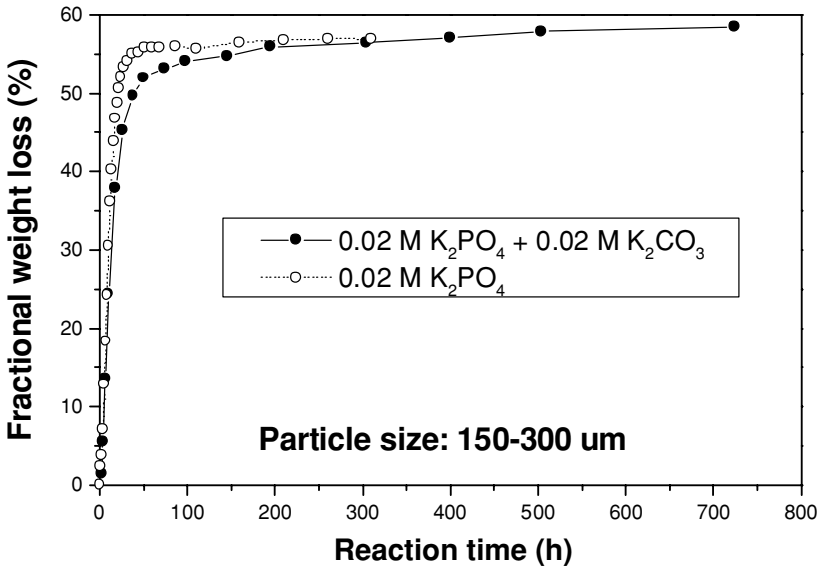

Fig. 10 Weight loss versus reaction time during conversion of the borate 3B glass to HA in a mixed solution of 0.02 M K_2HPO_4 and 0.02 M K_2CO_3 at 37°C and in a solution of 0.02 M K_2HPO_4 containing no K_2CO_3.

the Ca^{2+} ions from the glass to form stoichiometric HA, the theoretical PO_4^{3-} concentration in the four final solutions was calculated to be 230–350 μg/cm^3. The measured final concentrations were 300 μg/cm^3 for the solution resulting from the 3B glass reaction and ~400 μg/cm^3 for the solutions from the 0B, 1B, and 2B glass reactions.

For all four glasses, the Ca^{2+} concentration in the solution throughout the reaction was below the detection limit (<0.5 ppm) of the AA spectrometer. These data are in agreement with the observations of Richard [17], who found that K_2HPO_4 solutions with a wide range of concentrations (0.001–1 M) contained little Ca^{2+} after reacting with 0B or 3B glasses. The presence of boron in the solutions could not be accurately determined using the AA technique.

3.4. Carbonate-substituted hydroxyapatite

To study the formation of a carbonate-substituted HA, the four glasses were reacted in a mixed solution of 0.02 M K_2HPO_4 and 0.02 M K_2CO_3. Figs 10 and 11 show weight loss and pH data for the 3B glass (particle size 150–300 μm). For all four glasses, the data were almost identical to those for the reaction in just the 0.02 M K_2HPO_4 solution, indicating that the presence of K_2CO_3 at the present concentration in the solution had little effect on the conversion reaction. Figs 12 and 13 indicate that a carbonate-substituted HA was formed in the mixed solution. A comparison of these two spectra with those in Figs. 5 and 6 (for the product formed in just the K_2HPO_4 solution) showed no significant differences. It is

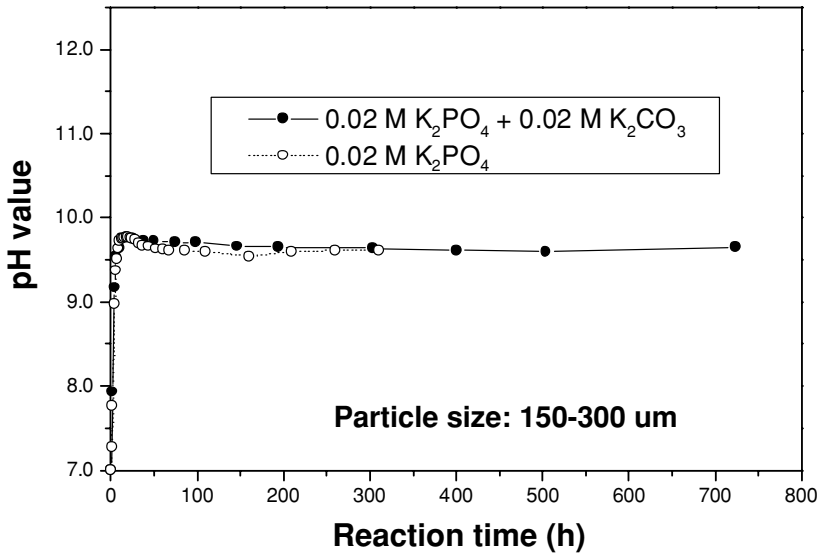

Fig. 11 pH of the solution versus reaction time during conversion of borate 3B glass to HA in a mixed solution of 0.02 M K_2HPO_4 and 0.02 M K_2CO_3 at 37°C and in a solution of 0.02 M K_2HPO_4 containing no K_2CO_3.

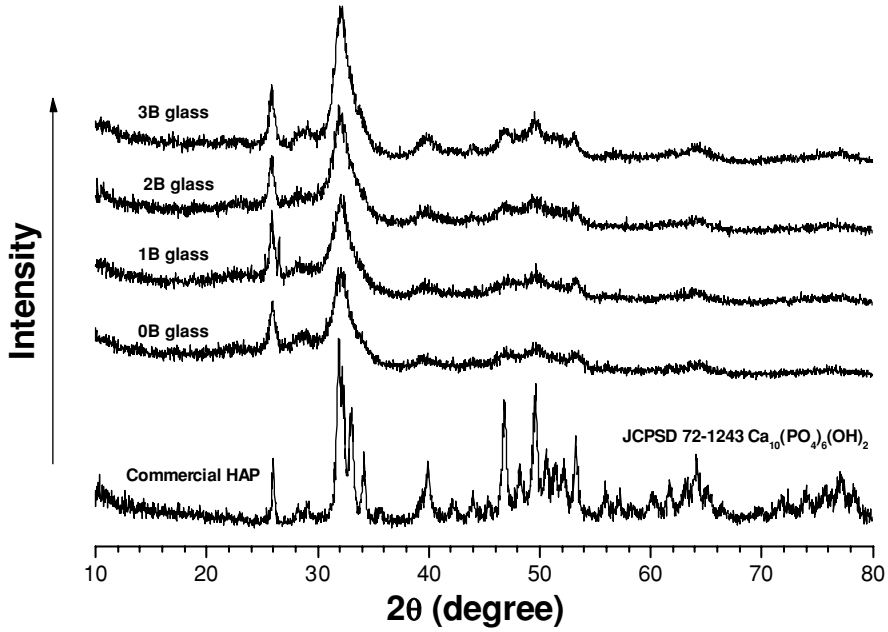

Fig. 12 XRD patterns of the products for 0B, 1B, 2B, and 3B glasses after reaction in a mixed solution of 0.02 M K_2HPO_4 and 0.02 M K_2CO_3 at 37°C. The patterns are for the "as-formed" HA. For comparison, the pattern for a standard HA is also shown.

likely that dissolution of CO_2 from the atmosphere into the K_2HPO_4 solution provided a sufficiently high CO_3^{2-} concentration to produce a carbonate-substituted HA, so adding K_2CO_3 (at 0.02 M concentration) to the solution had little additional effect.

3.5. Mechanisms of glass conversion to hydroxyapatite

Upon immersion of the glasses into the phosphate solution, dissolution of components such as Na_2O, SiO_2, and B_2O_3 into the solution to form Na^+, BO_3^{3-}, and SiO_4^{4-} ions, coupled with reaction of Ca^{2+} ions from the glass with PO_4^{3-} from the solution to precipitate of HA on the glass, leads to weight loss of the glass. Weight loss measurements therefore provide a convenient parameter to monitor the conversion kinetics of the glasses to HA. The weight loss data in Fig. 1 indicate that as the SiO_2 in the 0B glass is replaced with B_2O_3 to give the 1B, 2B, and 3B compositions, the rate of conversion to HA increases. The more rapid conversion rate with increasing B_2O_3 content results from structural changes in the glass brought about by replacing SiO_2 with B_2O_3. Because of its three-fold coordination number, B cannot fully

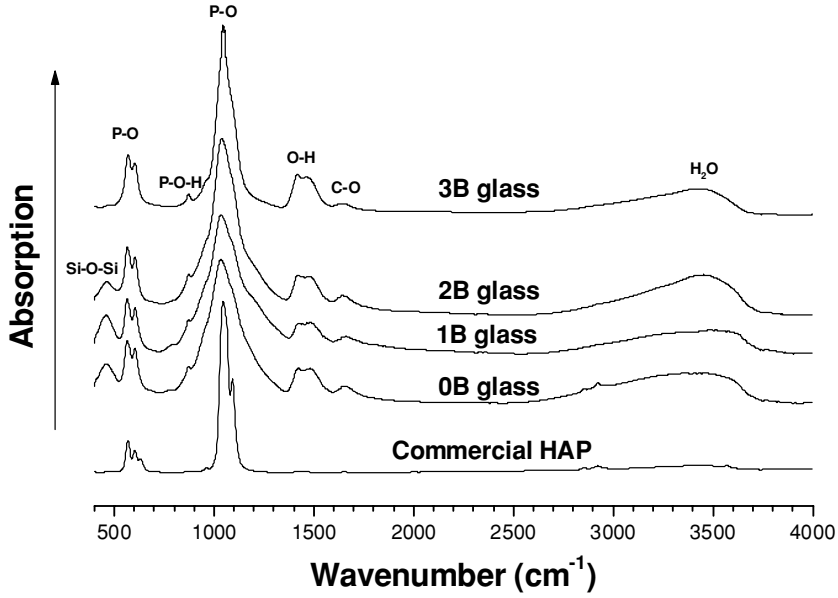

Fig. 13 FTIR patterns of products for 0B, 1B, 2B, and 3B glasses after reaction in a mixed solution of 0.02 M K_2HPO_4 and 0.02 M K_2CO_3 at 37°C. For comparison, the spectrum of a commercial HA is also shown.

form a three-dimension network when compared to Si, so therefore the borate glass has a lower chemical durability and, hence, a faster dissolution rate.

If it is assumed that all the Na_2O, B_2O_3, and SiO_2 in the glass dissolves completely into solution, and that only the CaO and P_2O_5 in the glass react with PO_4^{3-} ions in the solution to form stoichiometric HA, the theoretical weight loss, ΔW_{th}, is calculated to be 56.1, 57.2, 58.2, and 59.2 wt% for the 0B, 1B, 2B, and 3B glasses, respectively. Fig. 1 reveals that for the borate (3B) glass, a composition that contains no SiO_2, the measured limiting weight loss, $\Delta W_{lim} \approx 57.0$ wt%, is close to ΔW_{th}, indicating almost full conversion of this glass to HA. Full conversion of the 3B glass is also supported by chemical data obtained from EDS and XRF (Table 2), which indicate that CaO and P_2O_5 are the only major components in the reaction product. Furthermore, the Ca/P atomic ratio of the product, determined from both the EDS and XRF data is 1.7, which is almost identical to the value of 1.67 for stoichiometric HA.

For the silicate and borosilicate glasses, 0B, 1B, and 2B, the measured ΔW_{lim} is well below the theoretical value ΔW_{th}, indicating the possibility of incomplete conversion to HA. Evidence for incomplete conversion of these three glasses to HA is also found from EDS, XRF, and FTIR data for the reaction products. EDS and XRF indicate that, in addition to CaO and P_2O_5, SiO_2 is a major component of the reaction products. Since HA contains only CaO and P_2O_5, the EDS and XRF data indicate the presence of an unconverted, SiO_2-containing mass in addition to HA. FTIR spectra (Fig. 6) show Si–O bond resonance in the products of the 0B, 1B, and 2B glasses (but not in the 3B product), which also indicates the presence of Si.

For the 0B glass, the observed weight loss, $\Delta W_{lim} = 40\%$, and EDS, XRF, and AA data all indicate that Na_2O is completely dissolved from the glass. Using these two observations, it is calculated that ~50 wt% of the glass has reacted to form HA, leaving an unconverted core. Furthermore, based on this 50 wt% conversion to HA, the calculated concentrations of SiO_2, CaO, and P_2O_5 are 38, 41, and 21 wt%, respectively, and the calculated Ca/P atomic ratio is 2.5. These calculated values are not drastically different from the measured values from the XRF data in Table 2. In practice, because of the high pH of the solution and the increasing solubility of silica at pH values above 9–10 [30], some SiO_2 dissolution from the unconverted core would be expected to occur, making the actual SiO_2 content of the product somewhat lower than the calculated value.

The data therefore strongly indicate that for the 0B glass, the reaction stops well before complete conversion of the glass to HA. The glass–forming content of the 0B glass is less than 50%, so the structure of the glass is not strong enough to prevent the diffusion of Na^+ in the structure. As a result, Na^+ dissolution apparently continues until almost all the Na_2O in the glass dissolves into the solution, leaving a Na-depleted core, consisting of SiO_2, CaO, and P_2O_5.

For the borosilicate glass compositions (1B and 2B), which contain significant amounts of B_2O_3, a problem is that the B_2O_3 contents of the reaction products and the solutions cannot be measured by the EDS, XRF, and AA techniques used in this work. However, the data in Fig. 1 and Table 2 indicate that ΔW_{lim} and the Ca/P atomic ratio for these two glasses are not drastically different from the values for the 0B glass. Further work is being performed to better understand the conversion mechanisms in the 1B and 2B glasses, but at this stage, it would be useful to assume a reaction model similar to that described above for the 0B glass and examine the consequences arising from the B_2O_3.

Two extreme cases can be considered: (i) none of the B_2O_3 in the unconverted core dissolves into solution, and (ii) all the B_2O_3 in the unconverted core dissolves. In the former case, the weight loss and Ca/P atomic ratio would be approximately the same as the values determined for the 0B glass. However, the calculated SiO_2 content of the reaction products (23 wt% for 1B, and 12 wt% for 2B) would be well below the measured values (38.3 wt% and 25.6 wt%, respectively). In the latter case, if all the B_2O_3 simply dissolves out of the unconverted core, calculated weight loss and composition of the product are drastically different from the measured values.

For the 1B and 2B glasses, a third possibility is that the B_2O_3 in the unconverted core dissolves completely or partially into the solution but the dissolution of B_2O_3 is accompanied by some compensating effect, such as the incorporation of PO_4^{3-} or SiO_4^{4-} ions (or both species) into the unconverted core. For example, if charge balance is maintained in the structure of the unconverted core, four BO_3^{3-} units in the structure of the unconverted core are exchanged for three SiO_4^{4-} units from the solution. In this case, assuming that ~50% of the glass is converted to HA, as found for the 0B glass, the calculated compositions of the product, particularly the SiO_2 content, are not drastically different from the XRF data in Table 2.

Based on the data obtained in this work, the mechanisms by which the borate (3B) and silicate (0B) convert to HA in a dilute phosphate solution are summarized in Fig. 14. For the borate glass, dissolution of Na^+ (and presumably Ca^{2+}) from the glass into the solution occurs and at the same time the B–O network structure of the glass is attacked by phosphate solution. Immediately, the PO_4^{3-} ions from the solution react with Ca^{2+} ions, leading to nucleation and growth of HA, presumably at the more favorable Ca^{2+} sites located on the glass surface. The precipitated HA is highly porous, providing for easy ionic transport through it. The continuation of the dissolution–precipitation reactions leads to thickening of

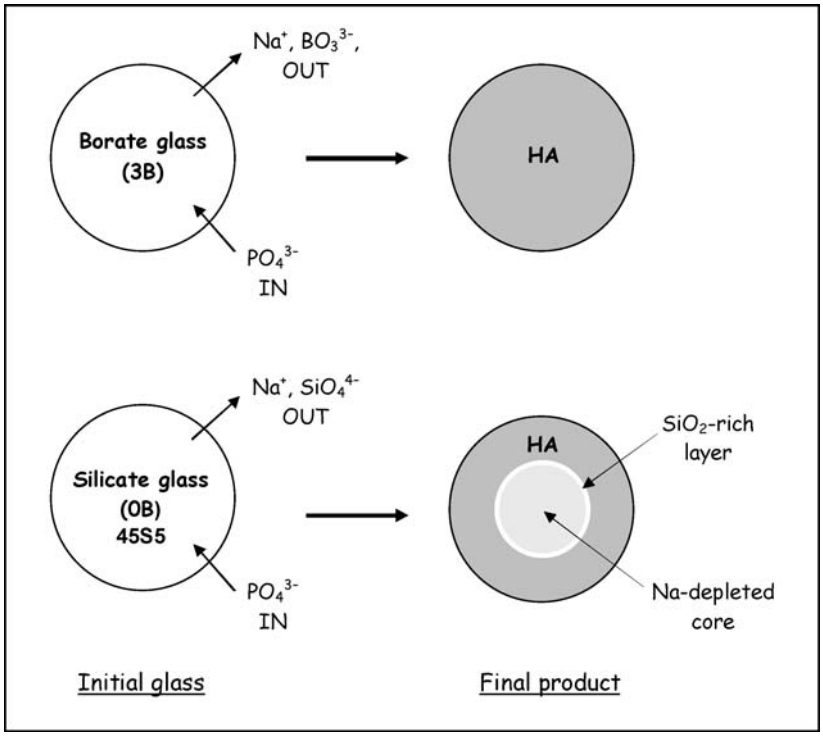

Fig. 14 Schematic diagram illustrating the mechanisms of conversion of a borate (3B) glass and 45S5 silicate (0B) glass to HA in a dilute phosphate solution.

the product layer from the surface of the particle inward. For the borate glass, this process continues until the glass is completely converted to HA.

For the silicate 0B glass (45S5), the initial steps in the conversion to HA are described by Hench [4, 5]. A porous SiO_2-rich gel layer forms and separates the growing HA layer from the shrinking glass core. For the reaction to continue, ions from the glass core must dissolve and diffuse through the SiO_2-rich layer. The data of this work show that, although the initial PO_4^{3-} concentration in the solution was sufficiently high to react with all the Ca^{2+} in the glass to form HA, the reaction effectively stopped well before the complete conversion to HA. The dissolution of SiO_2-rich gel layer depended on the pH value of the solution. At a certain pH value, the dissolution of the SiO_2-rich layer stopped when the saturation concentration of SiO_4^{4-} in the solution was reached.

For the borosilicate glasses (1B and 2B), a process similar to that described for the silicate 0B glass may occur, but for these two glasses, the consequences of the B_2O_3 in the unconverted core are not very clear at present. The techniques used in this work are not sensitive to B. Further work is in progress to provide further insight into the conversion mechanisms.

4. Conclusion

Replacing the SiO_2 in the silicate-based 45S5 bioactive glass with varying amounts of B_2O_3 produced glasses with controllable conversion rates to HA upon immersion in a dilute (0.02 M) K_2HPO_4 solution at near body temperature. Higher B_2O_3 content of the glass produced a more rapid conversion to HA, and a lower pH value of the phosphate solution. Particles of a borate glass (3B) (150–300 μm) were fully converted to HA in less than 4 days, whereas particles of 45S5 glass (0B) and two intermediate borosilicate compositions (1B and 2B), with the same size, were only partially converted even after 70 days. The unconverted core of the 0B, 1B, and 2B glasses contained a significant concentration of residual SiO_2 but all the Na_2O had dissolved. During the conversion to HA, the weight loss of the glass and the pH of the phosphate solution showed a similar dependence on time, indicating that they were controlled by the same processes. The structure and composition of the HA product were not strongly dependent on the composition of the glasses. The presence of a low concentration of CO_3^{2-} ions (0.02 M) in the phosphate solution produced a carbonate-substituted HA but had no effect on the kinetics of conversion to HA.

Acknowledgment Partial support for the work was provided by the University of Missouri Research Board (to MNR). The authors would like to thank Dr. L. Wang from MO-SCI Corp., Rolla, MO, for XRF analysis, Dr. H. Shi from CEST, UMR for helpful discussions on measuring phosphate ion concentration by the IC method, and Prof. S. Kapila, Department of Chemistry and CEST, UMR, for helpful discussions and for making AA and IC facilities available for the work.

References

1. L. L. HENCH, R. J. SPLINTER, W. C. ALLEN and T. K. GREENLEE, JR., *J. Biomed. Mater. Res.* **2** (1971) 117.
2. L. L. HENCH and J. WILSON, *Science* **226** (1984) 630.
3. L. L. HENCH, in Handbook of Bioactive Ceramics, edited by T. YAMAMURO, L. L. HENCH and J. WILSON (CRC Press, Boca Raton, FL, 1990) Vol. 1, p. 7.
4. L. L. HENCH, *J. Am. Ceram. Soc.* **74** (1991) 1487.
5. L. L. HENCH, *J. Am. Ceram. Soc.* **81** (1998) 1705.
6. T. NAKAMURA, T. YAMAMURO, S. HIGASHI, T. KOKUBO and S. ITO, *J. Biomed. Mater. Res.* **19** (1985) 685.
7. U. GROSS and V. STRUNZ, *J. Biomed. Mater. Res.* **19** (1985) 251.
8. W. HOELAND, W. VOGEL, K. NAUMANN, and J. GUMMEL, *J. Bomed. Mater. Res.* **19** (1985) 303.
9. T. KOKUBO, S. SAKKA and T. YAMAMURO, *J. Mater. Sci.* **21** (1986) 536.
10. S. YOSHII, Y. KAUTANI, T. YAMAMURO, T. NAKAMURA, T. KITSUGI, M. OKA, T. KOKUBO and M. TAKAGI, *J. Biomed. Mater. Res.* **22** (1988) 327.
11. T. KITSUGI, T. YAMAMURO and T. KOKUBO, *J. Bone Joint Surg.* **71** (1989) 264.
12. K. H. KARLSSON, H. FROBERG and K. RINGBOM, *J. Non-Cryst. Solids* **112** (1989) 69.
13. T. KOKUBO, H. KUSHITANI, S. SAKKA, T. KITSUGI and T. YAMAMURO, *J. Biomed. Mater. Res.* **24** (1990) 721.
14. S. D. CONZONE, R. F. BROWN, D. E. DAY and G. J. EHRHARDT, *J. Biomed. Mater. Res.* **60** (2002) 260.
15. D. E. DAY, J. E. WHITE, R. F. BROWN and K. D. MCMENAMIN, *Glass Technol.* **44** (2003) 75.
16. Q. WANG, W. HUANG, D. WANG, B. W. DARVELL, D. E. DAY and M. N. RAHAMAN, *J. Mater. Sci.: Mater. Med.* (2005), in press.
17. M. N. C. RICHARD, M. S. Thesis, University of Missouri-Rolla, 2000.
18. N. W. MARION, W. LIANG, G. REILLY, D. E. DAY, M. N. RAHAMAN and J. J. MAO, *Mech. Adv. Mater. Struct.* **12** (2005) 239.
19. L. L. HENCH and H. A. PASCHALL, *J. Biomed. Mater. Res. Symp.* **4** (1973) 25.
20. T. KOKUBO, S. ITO, Z. T. HUANG, T. HAYASHI, S. SAKKA, T. KITSUGIO and T. YAMAMURO, *J. Biomed. Mater. Res.* **24** (1990) 331.
21. P. DUCHEYNE, *J. Biomed. Mater. Res.* **21** (1987) 219.
22. J. A. WOJCIK, M. S. Thesis, University of Missouri-Rolla, 1999.
23. G. BORDAS and C. C. TRAPALIS, *J. Sol-Gel Sci. Technol.* **9** (1997) 305.
24. S. MATSUYA and Y. MATSUYA, *J. Mater. Sci.: Mater Med.* **9** (1998) 325.
25. H. MORGAN, R. M. WILSON, J. C. ELLIOTT, S. E. P. DOWKER and P. ANDERSON, *Biomaterials* **21** (2000) 617.
26. X. LU and Y. LENG, *Biomaterials* **26** (2005) 1097.
27. A. S. POSNER, N. C. BLUMENTHAL and F. BETTS, in Phosphate Minerals, edited by J. O. Nriagu and P. B. Moore (Springer-Verlag, Berlin, 1984) p. 331.
28. R. Z. LEGEROS and J. P. LEGEROS, in Phosphate Minerals, edited by J. O. Nriagu and P. B. Moore (Springer-Verlag, Berlin, 1984) p. 351.
29. J. BARRALET, S. BEST and W. BONFIELD, *J. Biomed. Mater. Res.* **41** (1998) 79.
30. R. K. ILER, in The Chemistry of Silica (Wiley, New York, 1979).